

“Sea Diamond” Wreckage—12 Years after the Fatal Maritime Accident, the Vessel Remains an Environmental Concern

Stephanos D. V. Giakoumatos , Efstratios N. Kalogirou

School of Maritime and Industrial Studies, University of Piraeus, 80, M. Karaoli & A. Dimitriou St., 18534 Piraeus, Greece

Email: *sgiakou@hotmail.com, *sgiakoum@unipi.gr, ozone.greece@gmail.com

How to cite this paper: Giakoumatos, S.D.V. and Kalogirou, E.N. (2020) “Sea Diamond” Wreckage—12 Years after the Fatal Maritime Accident, the Vessel Remains an Environmental Concern. *Open Journal of Ecology*, 10, 537-570.
<https://doi.org/10.4236/oje.2020.108034>

Received: June 10, 2020

Accepted: August 15, 2020

Published: August 18, 2020

Copyright © 2020 by author(s) and Scientific Research Publishing Inc. This work is licensed under the Creative Commons Attribution International License (CC BY 4.0).

<http://creativecommons.org/licenses/by/4.0/>



Open Access

Abstract

The present study was accomplished to fulfill the requisition of the Appeal Court of the city of Piraeus. According to the Court’s Decision, an environmental impact assessment should be made for the ongoing condition of the wreckage along with a study of the corrosion evolution process and a provision of the hull’s endurance should be estimated. The wreckage was sounded out, surveyed thoroughly by means of an ROV device immersed ad hoc. Extended videos and photo shots were taken and the exact position of the vessel depicted analytically on a sea contour depth chart. Hull corrosion, sea column & sea bottom sediment sampling carried out for the analysis of hazardous compounds PAHs, TPHs, PCBs and heavy metals in June and July of 2019. Fish and oyster tissues were analyzed in the lab for heavy metals’ detection. A great concern was given for (Cd) & (Pb) concentration in sea column nearby wreck. A report of about 1000 pages of the methodology & results was handed over to the Appeal Court of which merely partial significant segments are presented herein. The technical report denotes that PCBs, PAHs, TPHs sea bed & sea column measurements nearby the wreck were, in general, low or below detectable level. As regards heavy metals concentration level in aquatic sea column, the results indicate that only in certain locations heavy metals *i.e.* (Pb) and (Ni) were measured above the detection limit and classified according to contamination factors from moderate to high contamination level and might attribute to the presence of the wreck in the close area. Contamination factor indices consolidate the approach that the hull presence in the bottom contributes to the environmental degradation of the “caldera” ecosystem. The vessel’s hull is expected to be wiped out in almost four hundred years period according to the applied corrosion model.

Keywords

Heavy Metals, Caldera, Thira Island, Salvage, Greek Archipelago, Wreckage

Removal

1. Introduction

M/S Cruiser Sea Diamond (former Bikra Princess) sank on April 6th, 2007 a few hundred meters away from the commercial harbour of “Athenio” in Santorini “Thera” island alias “Thira”, in “caldera” location, in “Athenio” bay. The day before the incident the vessel ran aground on reefs which resulted in a 20 m long crack to be formed at the ship’s hull stabilizer level. That caused seawater inflow to the lower decks in huge amounts. The wreckage was fatal, given that two of the passengers aboard are declared missing ever since.

The vessel incurred severe environmental pollution at least the first months after the occurrence of the naval accident. Oil spillage polluted the nearby coastline whilst antipollution experts attempted for a long time to constrain the pollutants’ fate with controversially results. Despite the strenuous efforts in 2009 to pump out marine fuel oil and lubricants contained in numerous ship’s tanks, the results were poor and significant quantities of oil sludge, lubricants, hydraulic fluids, marine fuel oil not to mention significant heavy metal quantities as structural part of electrical and electronic devices mounted on the ship, still remain to be removed in an indeterminate future period [1]. Ever since, in the vicinity of the wreckage, sea body column and sea basin sediment are being environmentally monitored by the Technical University of Crete [2] [3] and the National Centre of Marine Research (NCMR) [4] [5].

The present study was financed by the Greek Public Authorities and accomplished for the purposes of the Appeal Court decision of the city of Piraeus. The Court assigned a judicial technical report to be conducted so that a clear assessment to be made for the condition of the wreckage in environmental terms and the formulation of a prognosis of the corrosion evolution process along with the endurance of the hull before wiping out in the sea bottom. Two judicial environmental experts enlisted in First Instance Court Catalogues of Piraeus, coordinated a multi-disciplinary scientific team to visit the island of Thira. Prior to sampling and hull survey, an autopsy took place to evaluate the surrounding in the vicinity of the spot of the fatal sea accident.

2. Wreck Survey & Field Sampling in Caldera

2.1. Survey Materials & Methods

A group of scientists, the appointed judicial experts and certified chemical analysts¹ along with a group of ROV² & diving experts³ visited the location of the wreckage in the period from 7 to 9 of June, and 5 to 7 of July, 2019.

¹Envirolab P.C., Email: info1@envirolab.gr Website: <http://www.envirolab.gr/el-GR/>.

²Remotely Operated Underwater Vehicle.

³Planet Blue diving center, Email: info@planetblue.gr Website: <http://www.planetblue.gr/>.

A thorough underwater observation and partially inspection of “Sea Diamond” hull and super-structures took place by means of a highly maneuverable submerged robot, remotely operated (ROV) named “super Achilles” (Figure 1). The ROV was of observation class II, manufactured by COMEX S.A., with specifications to satisfy all IMCA standards. The vehicle, equipped with a main and an auxiliary camera of low brightness with wide angle lens 0.001 LUX, was connected to the surface supporting vessel with a single coaxial umbilical. Sensors and lights supplemented the equipment. An imaging sonar (Tritech, model ST525V) and two (2) real time video channels supporting a professional box Sony Effio™ 960 h @ 0.001 Lux (F1.2) video camera. The ROV was being operated by means of a surface control unit connected to a computer, (RS 232C), sending simultaneously heading, altitude and depth data (Ultra Short BaseLine system) *i.e.* underwater acoustic positioning. Four (4) asynchronous 3.5 HP thrusters transmit maneuverability of the overall 130 kg weight, (incl. a stainless-steel chassis structure) which supports the potentially achievable maximum speed of 3.5 knots.

All power needed is supplied by a transformer of 190/210/230/250 Volts output. The INOX skeleton is enforced with PVC foam framework to support surface floating and good buoyancy. Tsunamis 99 software deployed for vectorized navigation charts production of high quality by Navigation Dynamics. The seabed around the wreckage was depicted analytically by deploying a side sonar 675 kHz scanner of Tritech, (SeaKing Towfish model) along with a Tritech Seagnet Pro software. All the above-mentioned equipment was mounted on the vessel “Oceanis” (Figure 2).

2.2. Results of the Underwater Inspection

ROV Wreck Scanning & Mapping of the Sea Basin

A squared kilometer of the sea bottom basin was mapped out analytically and a final depiction of sea basin configuration and buoy anchorages was completed, (Figures 3-5). In (Figure 5), the exact location of the oil containment boom (black ring-shaped perimeter) is depicted along with the buoys (red spots on the surface and immersed) fastened down firmly with many anchorages, a necessity to ensure their steady position regardless wind direction.

Great emphasis was laid on the analytical buoys’ anchorage depiction of the offshore sustaining boom for pollution prevent reasons. The seabed of our interest is comprised mostly of clayey sediments and rocky formations.

The sea bottom at the wreck area, declines in NE-SW direction fluctuating between 11 to 16 degrees, parallel to the vessel position. Wreck coordinates are in WGS 84, (given the reference spot in the centre of the hull) 36°23.711N - 02°52.581E. The vessel is well deposited on the bottom, thereof is quite unlike to change its position given the low tilting of the seabed.

The stern of the ship is located 0.55 nm away from the port of Athenio. The hull is almost aligned with the sea bed isobaths and the coastline direction. The

ship lies on the axis 144 degrees SE astern and 324 degrees NW at bow/ahead. Sea bed inclination is directing southwest and fluctuates between 11 and 16 degrees. Cracks were reported, located on decks No 3 & 4 (Figure 6 & Figure 7). Vessel inclination is 7 degrees astern and 12 degrees to the starboard. The minimum depth above the ship bridge is 86 m. The maximum depth at the portside of the bow is 147 m. The water body temperature against the depth was measured by ROV embedded device. The results were deployed for the hull's corrosion model.

During the ship underwater inspection many big fragments of the superstructure of the vessel were scattered in a large area upstream from the hull's position in caldera, very close to the coastline, a serious indication that the vessel at the time it touched down, in a bottom up position, started sliding down along with the seabed configuration, turned to the starboard and rolled over before it takes its final almost upright position. Many deep trails on the sea bottom, upstream near the coastline, delineate the sliding course.



Figure 1. ROV "super Achilles" at a close range.



Figure 2. The supporting vessel "OCEANIS" in the port of Athinio (Thira island).

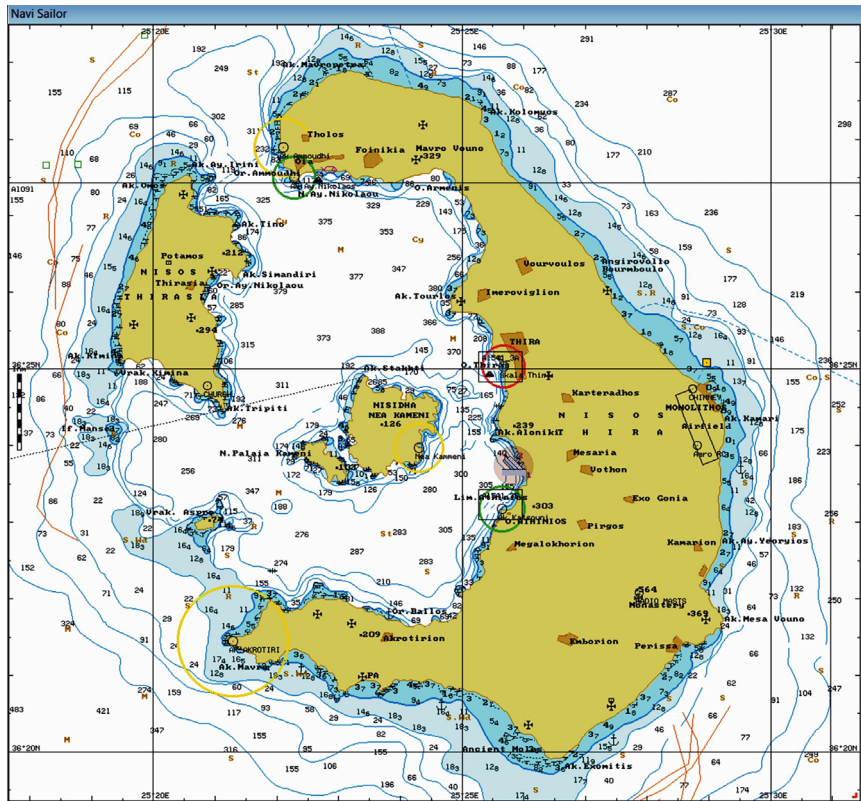


Figure 3. Nautical Chart of Santorini (Thira island) with depth contours.

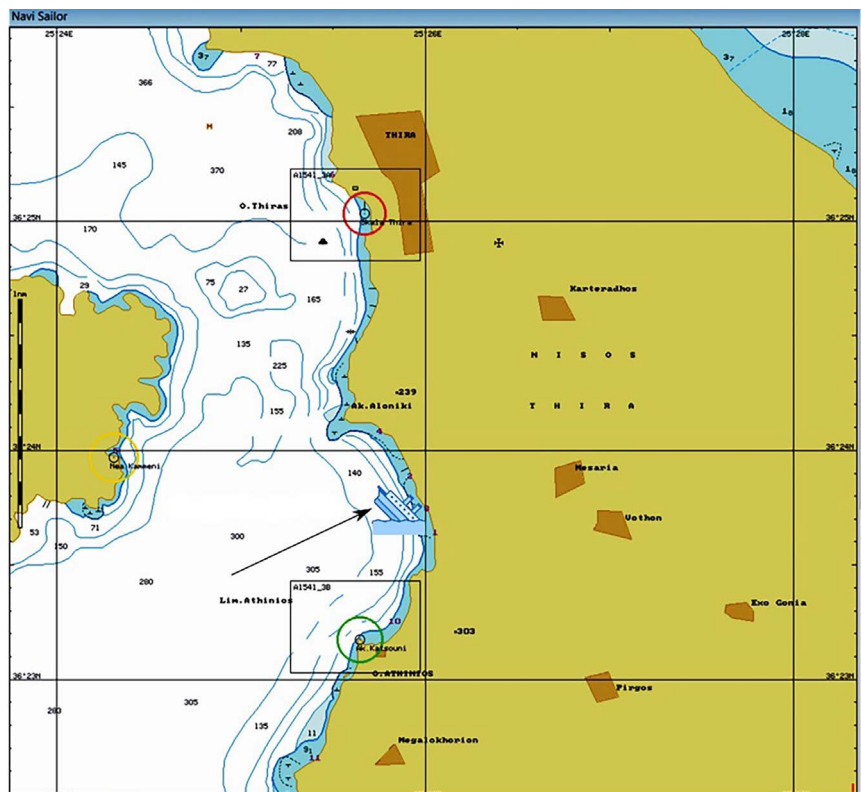


Figure 4. The exact location of M/S Sea Diamond hull, (enlarged chart), nearby Athenio harbour (Thira island).

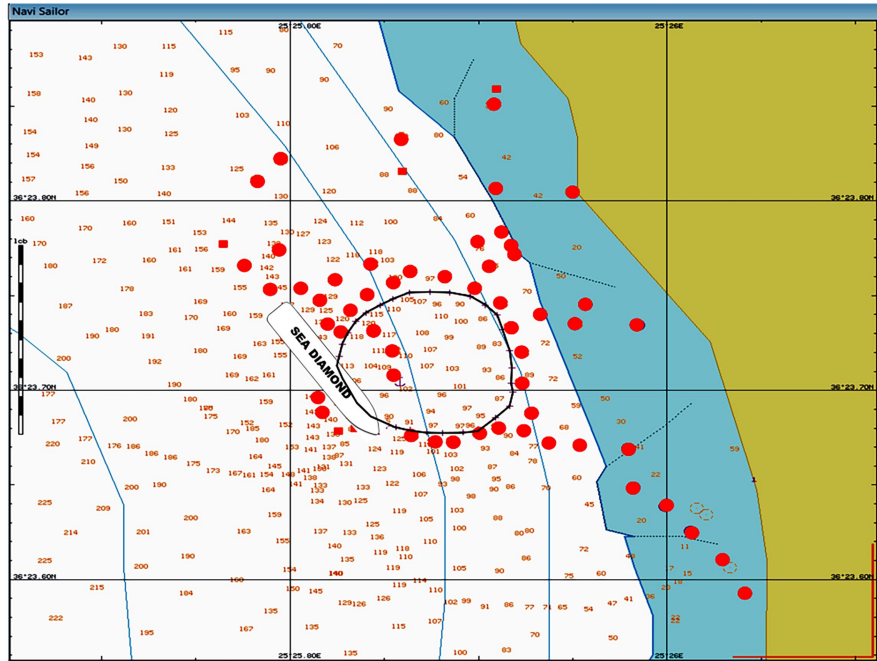


Figure 5. The exact location of M/S “Sea Diamond” along with the oil containment boom, (black ring-shaped perimeter) & buoys with anchorages for stabilization reasons (red spots).



Figure 6. Horizontal/longitudinal crack/rift of Deck #3 located in between structural transversal frame #114 and #137.



Figure 7. Vertical crack/rift of Deck #4 located at the transversal frame #138 on the port side (left side).

2.3. Materials & Methods of Sampling

Physicochemical parameters of the seawater column were measured by deploying a multi parameter seawater quality checker with the capacity of recording simultaneously within a range 0 to 30 m sea depth, the following measuring parameters: pH, Conductivity, (DO)⁴, Temperature, Depth, (TDS)⁵, Turbidity, Salinity, Seawater Specific Gravity and (ORP)⁶.

Sampling & Analyses' Protocols

The surface sampling of seawater was conducted by carrying out a Reach Pole Collection on 7th to 9th of June. Seawater sampling from certain sea depths were accomplished by using special Van Dorn & Ruttner sampling devices. Sea bed sediments were taken by using Ponar & Petersen grab samplers (**Figure 8**). Geographical coordinates (Lat, Lon) of each sample station are depicted on GPS panel device through an RS232 connection by means of a special Interface U2001 compatible with the NMEA-0183 Ver 2.0 protocol. Sampling team was comprised by accredited scientists in conformity with international protocols in sampling and sample handling (see **Table 1**).

Samples' pretreatment was according to US-EPA, (Method 3050B) regarding (Fe, Zn, Pb, Cd, Cu) analysis [19]. For the rest of the metals e.g. Ni, Cr etc. The ASTM D4698-92 Rev. 2007 was adopted for the analyses of the samples. Duplicate analysis was conducted for every sample collected [20]. Total Chromium as well as 6-valent Chromium were both estimated by using HACH protocols, Method 8023, 8024 and LCK 313.



Figure 8. Grab sampler in action collecting seabed sediment (Thira island).

⁴Dissolved Oxygen.

⁵Total Dissolved Solids.

⁶Redox Potential.

Table 1. Handling & preservation protocols [6]-[18].

Sampling and sample handling & preservation protocols	
Guidance on the design of sampling programmes and sampling techniques	ISO 5667-1:2006
Guidance on the preservation and handling of water samples	ISO 5667-3:2003
Guidance on sampling of sludge	ISO 5667-13:2011
Guidance on quality assurance of environmental water sampling and handling	ISO 5667-14:2014
Guidance on the preservation and handling of sludge and sediment samples	ISO 5667-15:2009
Guidance on sampling from marine waters	ISO 5667-9:1992
Guidance on sampling of bottom sediments	ISO 5667-12:2017
Standard Practices for Nitric Acid Digestion of Solid Waste	ASTM D5198-17
Standard Practices for Sampling with a Dipper or Pond Sampler	ASTM D5358-93:2009
Standard Practices for Sampling with a Scoop	ASTM D5633-04:2016
Standard Practices for Sampling Liquids Using Bailers	ASTM D6699-16
Standard Practices for Sampling Liquids Using Grab and Discrete Depth Samplers	ASTM D6759-16
Standard Guide for Packaging and Shipping Environmental Samples for Laboratory Analysis	ASTM D6911-15

Other elements (Mn, Cu, Ni, Cr, As, V, Cd, Fe, Co, Cu, Pb) in water column were analyzed by using Continuum Source Electrothermal Atomic Absorption Spectrometry *i.e.* CS AAS and adopting APHA 3113A, B, C methodology [21]. Mercury (Hg) in water column analyzed by implementing ISO 17852:2016 cold vapour Atomic Fluorescence Spectrometry methodology [22]. Zinc (Zn) in water column analyzed by employing APHA 3111 B, and AAS technique with flame (see **Table 2** & **Table 3**) [23]. Arsenic (As) analyzed by implementing ISO 11969:1996 methodology which employs absorption spectrometry (hydride technique) [24].

For TOC estimation HACH 10129 protocol was adopted. Heavy molecular chain hydrocarbons derived from fuel oils, analyzed by APHA 5520 B/APHA 5520 F [25] and US-EPA, 1664 (2010) methodology [26].

Hydride Generation Atomic Absorption Spectrometry based on ISO 11969:1996 was employed for Arsenic analysis in tissues of aquatic specimens. Fish stock tissue analyses conducted by Als Labs in Czech Republic, internal

Table 2. Chemical analysis methodology of sea column samples.

TOXIC ELEMENT	APPLIED LAB METHOD/TECHNIQUE
(Ni)	APHA ⁷ 3111B (Electrothermal CS AAS)
(Cu)	APHA 3111B (Electrothermal CS AAS)
(Zn)	APHA 3111B (Flame AAS)
(Pb)	APHA 3111B (Electrothermal CS AAS)
(Cd)	APHA 3111B (Electrothermal CS AAS)
(Fe)	APHA 3111B (Electrothermal CS AAS)
(Cr)	APHA 3111B (Electrothermal CS AAS)
(Mn)	APHA 3111B (Electrothermal CS AAS)
(Hg)	ISO 17852:2016 (CV-AFS)
(As)	ISO 11969:1996 (ET-CS-HRAAS)
(V)	APHA 3111B (Electrothermal CS AAS)

Table 3. Chemical analysis methodology of sea bed sediment sampling and aquatic species fish stock tissues.

TOXIC ELEMENT	APPLIED LAB METHOD/TECHNIQUE
(Ni)	APHA 3111B (Flame AAS)
(Cu)	APHA 3111B (Flame AAS)
(Zn)	APHA 3111B (Flame AAS)
(Pb)	APHA 3111B (Flame AAS)
(Cd)	APHA 3111B (Flame AAS)
(Fe)	APHA 3111B (Flame AAS)
(Cr)	APHA 3113A, B, C (Electrothermal CS AAS)
(Mn)	APHA 3111B (Flame AAS)
(Hg)	ISO 17852:2016 (CV-AFS)
(As)	APHA 3113A, B, C (Electrothermal CS AAS)

methodological procedures applied based on ČSN EN ISO 9377-2 and the following given standards *i.e.* US EPA methods 8015D/8015C, US EPA method 3510C & TNRC Method 1006 [27] [28] [29] [30] [31]. Maximum acceptable levels are given in accordance to Greek and European legislation 98/83/EC & amendments [32]. In (Table 4) Lab's methodology & applied techniques to certain chemical agents are presenting.

PAHs of our interest were 16 overall compounds (e.g., Anthracene, Pyrene,

⁷American Public Health Association.

Fluorene etc.) (see **Table 5**). Their analyses were carried out by means of a Gas Chromatography with a Mass Spectrometer (GC-MS) or even more accurately by deploying an accurate multiplex gas chromatography-tandem mass spectrometry (GC-MS-MS) configuration, in conformity with US EPA method 8270E, ČSN EN ISO 6468 and US EPA method 8000D standards (see **Table 4**, **Table 5**) [36] [37] [38].

PCBs detection of a sampling series was accomplished in Als Czech Republic s.r.o.⁸ laboratories, by implementing internal operational methods in accordance with DIN 38407-3 and US EPA 8082A methodology (see **Table 6**). TPHs in sea water column samples were to be detected according to the methodology and lab techniques given (see **Table 7**) [39].

Table 4. Chemical analyses of sea column [33]-[35].

CHEMICAL AGENTS	APPLIED LAB METHOD/TECHNIQUE
TPHs ⁹	ISO 9377-2:2000/ČSN EN ISO 9377-2
PAHs ¹⁰	ISO 6468
PCBs ¹¹	DIN 38407-3

Table 5. Lab PAH applied lab method/technique.

PAHs	APPLIED LAB METHOD/TECHNIQUE
Naphtalene	Gas Chromatography coupled with Mass Spectrometer (GC-MS) Or alternatively Multiplex Gas Chromatography-tandem mass spectrometry (GC-MS-MS)
Acenaphthylene	
Acenaphthene	
Fluorene	
Phenanthrene	
Anthracene	
Fluoranthrene	
Pyrene	
Ben(a)anthracene	
Chrysene	
Benzo(b)fluoranthene	
Benzo(k)fluoranthene	
Benzo(a)pyrene	
Indeno(123-cd)pyrene	
Benzo(g,h,i)perylene	
Dibenz(a,h)anthracene	

⁸Official Als labs website <http://www.alsglobal.cz/>.

⁹Total petroleum hydrocarbons..

¹⁰Polycyclic aromatic hydrocarbons

¹¹Polychlorinated biphenyls.

Table 6. Lab PCB applied lab method/technique.

PCBs	APPLIED LAB METHOD/TECHNIQUE
PCB 28	
PCB 52	
PCB 101	
PCB 118	DIN 38407-3 & US EPA 8082A
PCB 138	Gas Chromatography method with Electron Capture Detection (GC-ECD)
PCB 153	
PCB 180	

Table 7. Lab petroleum hydrocarbon applied lab method/technique.

Petroleum Hydrocarbon Fraction	LAB METHODOLOGY/DETECTION TECHNIQUE
C ₁₀ -C ₁₂	
C ₁₀ -C ₄₀	ČSN EN ISO 9377-2, US EPA 8015C, D, US EPA 3510C, TNRCC Method 1006
C ₁₂ -C ₁₆	Gas Chromatography method with Flame Ionization Detection (GC-FID)
C ₁₆ -C ₃₅	
C ₃₅ -C ₄₀	

From 4th to 6th of July, 2019 the aforementioned group revisited the wreckage for an extra sampling (**Figures 9-11**). In the vicinity of wreckage, adequate quantities of fish stock and scallops were captured and collected. Fishing tissues were assembled by means of fishing nets use. All aquatic species assembled, were conserved temporarily in isothermal portable box with ice into ziplocked bags and transferred into isolated chamber in a properly retrofitted van until their arrival in laboratory premises.

All heavy metals but Mercury were traced and quantified by means of high-resolution continuum source Atomic Absorption Spectrometry (AAS), ContA700 of Analytic Jena A.G. with flame or electrothermal atomization when appropriate. Mercury is traced and quantified by applying the cold vapour atomic fluorescence spectroscopy (Cold Vapour AFS) (see **Table 3**).

2.4. Materials & Methods of Sampling

2.4.1. Sea Bottom Sampling Results

US EPA provides analytical table Criteria of Maximum Concentration (CMC), and Criteria of Continuous Concentration (CCC), regarding the acute & chronic impact of heavy metals in aquatic life and specifically to seawater. In (**Table 8**) are given MCC/CCC values and conversion factors for dissolved metals [40].

References [41] [42], introduced seven classes of the geo-accumulation index (I_{geo}) (see Equation (1)) to identify the heavy metals' pollution magnitude in sediments. Values lower or equal to zero indicate practically non-polluted soil. On the other side, values greater than 5 indicate sediments extremely polluted. (**Table 9**) presents the pollution classes. (I_{geo}) calculation formula is given below:

Table 8. Maximum Concentration Criteria for seawater column in ($\mu\text{g}\cdot\text{L}^{-1}$) of certain pollutants.

Pollutant	Maximum Concentration	Continuous Concentration	Conversion Factor
Arsenic (As)	69.0	36.00	1.000
Cadmium (Cd)	33.0	7.90	0.994
Chromium (Cr) (VI)	1,100.0	50.00	0.993
Copper (Cu)	4.8	3.10	0.830
Lead (Pb)	140.0	5.60	0.951
Zinc (Zn)	90.0	81.00	0.946
Nickel (Ni)	74.0	8.20	0.990
Mercury (Hg)	1.8	0.94	0.850

Table 9. Geo-accumulation index (I_{geo}) pollution classes [42].

I_{geo}	Pollution characterization
>5	extremely polluted
4 - 5	strongly to extremely polluted
3 - 4	strongly polluted
2 - 3	moderately to strongly polluted
1 - 2	moderately polluted
0 - 1	unpolluted to moderately polluted
<0	unpolluted

$$I_{\text{geo}} = \log_2 \left(\frac{C_n}{1.5 * B_n} \right) \quad (1)$$

where (C_n) the measured conc. of element Pb and (B_n) the background preindustrial shale concentration of the same element. Each element has its own background shale/crust values. Geo-accumulation index (I_{geo}) in several sampling areas of our interest, in June & July of 2019, were estimated in (Table 10). Red coloured values indicate sampling spots of pollution concern.

Furthermore, according to [43] [44], US-EPA adopted indices *i.e.* contamination factor (CF) or (C_f) & pollution load index (PLI) and contamination levels, are presented in (Table 11) whereas in (Table 12), laboratory analyses' outcome is presented colourful when indicating remarkable contamination level is the case. The aforementioned indices were deployed to evaluate the contamination level of the sea bed nearby wreckage. (PLI) calculation formula (see Equation (2)), is given below:

$$\text{PLI} = (CF_1 * CF_2 * \dots * CF_m)^{1/m} \quad (2)$$

where m denotes a contamination factor.

An improved contamination index (mC_d) and altered contamination levels

were introduced (Table 13) [45] [46]. The improved contamination factor is given by the below written formula (Equation (3)):

$$mC_d = \frac{\sum_{i=1}^k CF^i}{k} \quad (3)$$

Table 10. Geo-accumulation Index gradation, on seabed sediments in caldera (Thira island), nearby “Sea Diamond” wreckage (June-July 2019).

GEOACCUMULATION INDEX							
sampling station	sampling date	$I_{geo,Cu}$	$I_{geo,Zn}$	$I_{geo,Cr}$	$I_{geo,Cd}$	$I_{geo,Pb}$	$I_{geo,Ni}$
Δ1→S1	5/7/2019	-2.58	-2.10	-3.74	2.22	0.71	-2.73
Δ2→S2	5/7/2019	-3.11	-3.00	-4.19	2.15	-1.54	-3.57
Δ3→S3	5/7/2019	-3.09	-2.10	-3.84	-5.49	0.58	-3.14
Δ4→S4	5/7/2019	-3.17	-2.90	-3.22	2.35	-1.18	-2.81
Δ5→S5	5/7/2019	-12.72	-5.48	-13.72	-5.49	-11.55	-13.32
Δ7→S7	5/7/2019	-3.25	-3.86	-13.72	-5.49	-1.16	-3.06
Δ8→S8	5/7/2019	-2.64	-2.83	-13.72	2.15	-11.55	-3.24
Δ9→S9	5/7/2019	-12.72	-3.72	-1.34	4.00	0.61	-0.73
Δ6→S6	5/7/2019	-12.72	-3.06	-4.40	-5.49	-1.42	-2.93
Δ1→S1	7/6/2019	-2.12	-2.96	-3.24	-5.49	-1.08	-3.60
Δ3→S3	7/6/2019	-2.01	-0.58	-3.84	3.83	1.54	-2.08
Δ13→S13	7/6/2019	-3.15	-4.92	-4.15	-5.49	-1.80	-3.71
Δ16→S16	7/6/2019	-2.62	-3.56	-3.68	-5.49	-2.37	-2.84
Δ17→S17	7/6/2019	-2.83	-3.52	-3.77	-5.49	-1.87	-3.20
Δ18→S18	7/6/2019	-2.43	-2.62	-3.73	-5.49	-1.32	-3.06
Δ20→S20	7/6/2019	-2.22	-2.54	-3.37	2.42	1.23	-2.64
Δ21→S21	7/6/2019	-2.55	-3.35	-3.96	2.29	-1.13	-3.25
	min	-12.72	-5.48	-13.72	-5.49	-11.55	-13.32
	max	-2.01	-0.58	-1.34	4.00	1.54	-0.73
	Mean	-2.92	-3.04	-3.63	1.80	-0.32	-2.78

Table 11. Soil contamination categories according to CF and PLI assessment [43] [44].

Contamination Factor (CF)	Contamination Level	PLI value	Contamination Level
CF < 1	Low	PLI < 5	Low
1 ≤ CF < 3	Moderate	5 < PLI < 50	Moderate
3 ≤ CF < 6	Considerable	50 < PLI < 100	Considerable
CF > 6	Very high	PLI > 100	Very high

Table 12. CF and PLI indices of seabed sediments in caldera (Thira island) nearby “Sea Diamond” wreckage (June-July 2019).

CONTAMINATION FACTOR (FC) AND POLLUTION LOAD INDEX (PLI)											
sampling station	sampling date	sampling depth (m)	CF _{Cu}	CF _{Zn}	CF _{Cr}	CF _{Ca}	CF _{Pb}	CF _{Ni}	CF _{Hg}	mC _d	PLI
Δ1→S1	5/7/2019	11	0.23	0.44	0.10	10.50	3.51	0.19	0.00	2.14	0.64
Δ2→S2	5/7/2019	100	0.16	0.24	0.07	10.00	0.74	0.11	0.00	1.62	0.36
Δ3→S3	5/7/2019	103	0.16	0.44	0.09	0.05	3.20	0.15	0.00	0.58	0.23
Δ4→S4	5/7/2019	10	0.15	0.25	0.15	11.50	0.94	0.18	0.00	1.88	0.47
Δ5→S5	5/7/2019	5	0.00	0.04	0.00	0.05	0.00	0.00	0.00	0.01	0.00
Δ7→S7	5/7/2019	10	0.14	0.13	0.00	0.05	0.96	0.15	0.00	0.20	0.05
Δ8→S8	5/7/2019	5	0.22	0.27	0.00	10.00	0.00	0.14	0.00	1.52	0.04
Δ9→S9	5/7/2019	5	0.00	0.14	0.53	36.00	3.28	0.77	0.00	5.82	0.33
Δ6→S6	5/7/2019	5.5	0.00	0.23	0.06	0.05	0.80	0.17	0.00	0.19	0.05
Δ1→S1	7/6/2019	11	0.31	0.24	0.14	0.05	1.01	0.11	0.00	0.27	0.20
Δ3→S3	7/6/2019	100	0.34	1.27	0.09	32.00	6.23	0.30	0.00	5.75	1.16
Δ13→S13	7/6/2019	103	0.15	0.06	0.08	0.05	0.61	0.10	0.00	0.15	0.11
Δ16→S16	7/6/2019	10	0.22	0.16	0.11	0.05	0.41	0.18	0.00	0.16	0.15
Δ17→S17	7/6/2019	5	0.19	0.17	0.10	0.05	0.59	0.14	0.00	0.18	0.15
Δ18→S18	7/6/2019	10	0.25	0.31	0.10	0.05	0.86	0.15	0.00	0.25	0.19
Δ20→S20	7/6/2019	5	0.29	0.33	0.13	12.00	5.04	0.21	0.00	2.57	0.73
Δ21→S21	7/6/2019	5	0.23	0.19	0.09	11.00	0.98	0.13	0.00	1.80	0.42
		min	0.00	0.04	0.00	0.05	0.00	0.00	0.00	0.01	0.00
		max	0.34	1.27	0.53	36.00	6.23	0.77	0.00	5.82	1.16
		Mean	0.18	0.23	0.11	7.85	1.72	0.19	0.00	1.48	0.31

Table 13. Modified contamination degrees [45] [46].

Index value	Contamination classes [2]
$mC_d < 1.5$	Nil to very low degree
$2.0 \leq mC_d < 4.0$	Moderate degree
$4.0 \leq mC_d < 8.0$	High degree
$8.0 \leq mC_d < 16.0$	Very high degree
$16.0 \leq mC_d < 32.0$	Extremely high degree
$mC_d \geq 32.0$	Ultra-high degree

where: (*k*) the number of analyzed elements (heavy metals) and (*i*) a pollutant. The remote sampling station (S7) was elected, on purpose, to serve as a reference (unbiased) location.

2.4.2. Sea Column Sampling Results

The following tables present the overall results of the analysis of sea column samples, the pollutants to be measured (heavy metals and organic compounds

i.e. TPHs, PAHs, PCBs) and the exact location of various sampling stations. Totally 11 pollutants (heavy metals) were analyzed of which only four are given in (Table 14) since the unlisted ones were below the detection level. Organic pollutants' results are presented in (Table 15).

Table 14. Results for sea column sampling for pollutants above detection level, N.D. (Not Detected).

Location	(Cu) ($\mu\text{g}\cdot\text{L}^{-1}$)	(Fe) ($\mu\text{g}\cdot\text{L}^{-1}$)	(Pb) ($\mu\text{g}\cdot\text{L}^{-1}$)	(Ni) ($\mu\text{g}\cdot\text{L}^{-1}$)
S1 Sea Surface (36'23.655N, 25'26.042E)	N.D.	12.6	N.D.	N.D.
S1 Sea column, (11 m) (36'23.655N, 25'26.042E)	N.D.	11.4	N.D.	N.D.
C3b Sea surface (inbound offshore booms) (36'23.712N, 25'25.917E)	N.D.	21.4	3.0	5.9
S3 Sea surface (36'23.704N, 25'25.856E)	N.D.	8.9	N.D.	N.D.
S3 Sea sample, (95 m) (36'23.704N, 25'25.856E)	N.D.	10.6	N.D.	N.D.
S12 Sea surface (36'23.712N, 25'25.880E)	N.D.	14.3	N.D.	N.D.
S12 Sea column, (85 m) (36'23.712N, 25'25.880E)	N.D.	15.6	N.D.	N.D.
S12 Sea surface (36'23.712N, 25'25.880E)	N.D.	17.6	N.D.	N.D.
S12 Sea column, (103 m) (36'23.712N, 25'25.880E)	N.D.	14.4	N.D.	N.D.
S13 Sea surface (36'23.831N, 25'25.941E)	N.D.	14.9	N.D.	N.D.
S13 Sea column, (10 m) (36'23.831N, 25'25.941E)	N.D.	17.0	2.0	N.D.
S14 Sea surface (36'23.744N, 25'25.861E)	N.D.	21.0	N.D.	N.D.
S14 Sea column, (80 m) (36'23.744N, 25'25.861E)	N.D.	14.0	N.D.	N.D.
S15 Sea surface (36'23.734N, 25'25.906E)	N.D.	13.1	N.D.	N.D.
S15 Sea column, (93 m) (36'23.734N, 25'25.906E)	N.D.	12.7	2.0	N.D.
S16 Sea surface (36'23.905N, 25'25.912E)	N.D.	15.6	N.D.	N.D.
S16 Sea column, (10 m) (36'23.905N, 25'25.912E)	N.D.	15.4	N.D.	N.D.
S17 Sea surface (36'23.889N, 25'25.920E)	N.D.	11.8	N.D.	N.D.
S17 Sea column, (18 m) (36'23.889N, 25'25.920E)	N.D.	12.4	N.D.	N.D.
S18 Sea surface (36'23.776N, 25'25.971E)	N.D.	19.5	N.D.	N.D.
S18 Sea column, (10 m) (36'23.776N, 25'25.971E)	N.D.	14.3	N.D.	N.D.
S19 Sea surface (36'23.771N, 25'25.924E)	3,1	12.8	N.D.	N.D.
S19 Sea column, (55 m) (36'23.771N, 25'25.924E)	N.D.	11.0	N.D.	N.D.
S20 Sea column, (2 m) (36'23.686N, 25'26.014E)	N.D.	10.6	N.D.	12.0
S21 Sea column, (66 m) (36'23.665N, 25'25.831E)	N.D.	16.6	N.D.	N.D.
S21 Sea column, (131 m) (36'23.665N, 25'25.831E)	N.D.	15.2	N.D.	N.D.
S22 Sea column, (40 m) (36'23.825N, 25'25.068E)	N.D.	9.9	2.0	N.D.
S22 Sea column, (55 m) (36'23.825N, 25'25.068E)	N.D.	12.4	N.D.	5.1
S23 Sea column, (35 m) (36'24.048N, 25'25.073E)	N.D.	8.8	N.D.	N.D.
S24 Sea surface (36'23.421N, 25'25.0718E)	N.D.	15.3	N.D.	N.D.
S24 Sea column, (100 m) (36'23.421N, 25'25.071E)	N.D.	15.4	N.D.	N.D.
S25 Sea surface (36'23.263N, 25'25.805E)	N.D.	8.6	N.D.	N.D.
S25 Sea column, (4 m) (36'23.263N, 25'25.805E)	N.D.	12.4	N.D.	N.D.

Table 15. Results for sea column sampling for three main pollutant categories *i.e.* TPHs, PAHs, PCBs in July, 2019, N.D. (Not Detected).

Location	TPH ($\mu\text{g}\cdot\text{L}^{-1}$)	PAHs ($\mu\text{g}\cdot\text{L}^{-1}$)	PCBs ($\mu\text{g}\cdot\text{L}^{-1}$)
S1 Sea Surface (36°23.655N, 25°26.042E)	N.D.	N.D.	N.D.
S1 Sea column (11 m) (36°23.655N, 25°26.042E)	N.D.	N.D.	N.D.
C3b Sea surface (inbound offshore booms) (36°23.712N, 25°25.917E)	N.D.	N.D.	N.D.
S3 Sea surface (36°23.704N, 25°25.856E)	N.D.	N.D.	N.D.
S3 Sea sample, (95 m) (36°23.704N, 25°25.856E)	N.D.	N.D.	N.D.
S12 Sea surface (36°23.712N, 25°25.880E)	N.D.	N.D.	N.D.
S12 Sea column, (85 m) (36°23.712N, 25°25.880E)	N.D.	N.D.	N.D.
S12 Sea surface (36°23.712N, 25°25.880E)	N.D.	N.D.	N.D.
S12 Sea column, (103 m) (36°23.712N, 25°25.880E)	N.D.	N.D.	N.D.
S13 Sea surface (36°23.831N, 25°25.941E)	N.D.	N.D.	N.D.
S13 Sea column, (10 m) (36°23.831N, 25°25.941E)	N.D.	N.D.	N.D.
S14 Sea surface (36°23.744N, 25°25.861E)	N.D.	N.D.	N.D.
S14 Sea column, (80 m) (36°23.744N, 25°25.861E)	N.D.	N.D.	N.D.
S15 Sea surface (36°23.734N, 25°25.906E)	N.D.	N.D.	N.D.
S15 Sea column, (93 m) (36°23.734N, 25°25.906E)	N.D.	N.D.	N.D.
S16 Sea surface (36°23.905N, 25°25.912E)	N.D.	N.D.	N.D.
S16 Sea column, (10 m) (36°23.905N, 25°25.912E)	N.D.	N.D.	N.D.
S17 Sea surface (36°23.889N, 25°25.920E)	N.D.	N.D.	N.D.
S17 Sea column, (18 m) (36°23.889N, 25°25.920E)	N.D.	N.D.	N.D.
S18 Sea surface (36°23.776N, 25°25.971E)	N.D.	N.D.	N.D.
S18 Sea column, (10 m) (36°23.776N, 25°25.971E)	N.D.	N.D.	N.D.
S19 Sea surface (36°23.771N, 25°25.924E)	N.D.	N.D.	N.D.
S19 Sea column, (55 m) (36°23.771N, 25°25.924E)	N.D.	N.D.	N.D.
S20 Sea column, (2 m) (36°23.686N, 25°26.014E)	N.D.	N.D.	N.D.
S21 Sea column, (66 m) (36°23.665N, 25°25.831E)	N.D.	N.D.	N.D.
S21 Sea column, (131 m) (36°23.665N, 25°25.831E)	N.D.	N.D.	N.D.
S22 Sea column, (40 m) (36°23.825N, 25°25.068E)	N.D.	N.D.	N.D.
S22 Sea column, (55 m) (36°23.825N, 25°25.068E)	N.D.	N.D.	N.D.
S23 Sea column, (35 m) (36°24.048N, 25°25.073E)	N.D.	N.D.	N.D.
S24 Sea surface (36°23.421N, 25°25.0718E)	N.D.	N.D.	N.D.
S24 Sea column, (100 m) (36°23.421N, 25°25.071E)	N.D.	N.D.	N.D.
S25 Sea surface (36°23.263N, 25°25.805E)	N.D.	N.D.	N.D.
S25 Sea column, (4 m) (36°23.263N, 25°25.805E)	N.D.	N.D.	N.D.

Continued

Sea Surface (36°23.880N, 25°25.920E)	C10 - C12: <5.0	Naphthalene: 0.601	N.D.
	C10 - C40: 56.3		
	C12 - C16: <5.0		
	C16 - C35: 51.3		
	C35 - C40: <10.0		
Sea Surface (36°23.943N, 25°25.886E)	C10 - C12: 35.0	N.D.	N.D.
	C10 - C40: 19,300		
	C12 - C16: 42.1		
	C16 - C35: 10,400		
	C35 - C40: 8,851		

2.4.3. Fish Stock & Scallops' Sampling Results

Apart from sea bed sediment and sea column sampling, fish stock and scallops were fished and their tissues were undergone tests for pollutants. The lab results of tissue analyses were selected in (Table 16).

Simpson's Diversity Index (D) (see Equation (4)), is one of the most widely used and reliable to quantify biodiversity of a habitat of our interest. In fact, it represents the distribution variation of species abundance [47] [48]. The Index measures the probability that two individuals randomly sampled will belong to the same species (or some category other than our species).

$$D = \frac{\sum_{j=1}^S n_j * (n_j - 1)}{N * (N - 1)} \quad (4)$$

where (n_j) the number of entities of (j^{th}) species and (N) the total number of entities. (S) denotes the quantification of different species of a certain dataset (ecosystem) of our interest (Table 17).

A popular index in the scientific community is undoubtedly the widely known as Shannon-Wiever Index [49] (Table 17), to measure species in an ecosystem. The above index is based on Information Theory-Shannon Entropy that approaches and quantifies the uncertainty encountered, in predicting the species identity and not on applied ecological practices [50]. Diversity indices present a structural measurement of heterogeneity of bio-communities (datasets) in ecosystems.

Shannon Index (H') is estimated according to the given formula [48] (Equation (5)):

$$H' = -\sum_{w=1}^S p_w * \ln p_w \quad (5)$$

where (p_w) denotes the proportion of total sample represented by species (w) individual of a bio-community and (S) the number of species in the community.

Although Shannon index increases along with the number of species in an ecosystem and theoretically could reach very high values, in fact fluctuates between from 1.5 to 3.5, only in rare cases exceeds the value of 4 [48] [51] and seems not to exceed the value of 5 [50] [52].

Table 16. Results for (Fe, Zn, Mn & As) of aquatic species (fish stock) tissues from caldera nearby wreckage, N.D. (Not Detected).

Fish stock	(Fe) (mg·kg ⁻¹)	(Zn) (mg·kg ⁻¹)	(Mn) (mg·kg ⁻¹)	(As) (mg·kg ⁻¹)
Scorpeana porcus, demersal, (188 g, 210 mm)	N.D.	N.D.	N.D.	N.D.
Scorpeana porcus demersal, (145 g, 160 mm)	N.D.	1.4	N.D.	N.D.
Scorpeana porcus, demersal (69 g, 200 mm)	N.D.	N.D.	N.D.	N.D.
Phycis phycis, benthopelagic, (335 g, 325 mm)	N.D.	N.D.	N.D.	N.D.
Phycis phycis, benthopelagic, (197 g, 260 mm)	N.D.	N.D.	N.D.	N.D.
Phycis phycis, benthopelagic, (284 g, 325 mm)	N.D.	N.D.	N.D.	N.D.
Phycis phycis, benthopelagic, (201 g, 265 mm)	N.D.	N.D.	N.D.	N.D.
Phycis phycis, benthopelagic, (201 g, 280 mm)	N.D.	N.D.	N.D.	N.D.
Merluccius, merluccius, demersal, (269 g, 350 mm)	N.D.	1.0	N.D.	N.D.
Scorpaena scrofa, demersal, (92 g, 175 mm)	6.7	1.6	N.D.	N.D.
Scorpaena scrofa, demersal, (198 g, 230 mm)	7.4	1.4	N.D.	N.D.
Scorpaena scrofa, demersal, (116 g, 185 mm)	6.9	1.0	N.D.	N.D.
Scorpaena scrofa, demersal, (188 g, 210 mm)	7.8	1.2	N.D.	N.D.
Scorpaena scrofa, demersal, (145 g, 160 mm)	8.4	N.D.	N.D.	N.D.
Scorpaena scrofa, demersal, (69 g, 200 mm)	6.2	N.D.	N.D.	N.D.
Siganus luridus, reef fish, benthic, (75 g, 175 mm)	N.D.	N.D.	N.D.	N.D.
Simphodus ocellatus, reef fish, (315 g, 265 mm)	N.D.	1.4	N.D.	N.D.
Simphodus ocellatus, reef fish, (493g, 306 mm)	N.D.	N.D.	N.D.	N.D.
Simphodus ocellatus, reef, (105g, 195 mm)	N.D.	N.D.	N.D.	N.D.
Pagellus acarne, benthopelagic, (175 g, 220 mm)	5.7	1.8	N.D.	N.D.
Pagellus acarne, benthopelagic, (111 g, 230 mm)	N.D.	1.4	N.D.	N.D.
Pagellus acarne, benthopelagic, (124 g, 205 mm)	N.D.	1.2	N.D.	N.D.
Pagellus acarne, benthopelagic, (118 g, 210 mm)	5.6	1.7	N.D.	N.D.
Pagellus acarne, benthopelagic, (153 g, 240 mm)	N.D.	2.1	N.D.	N.D.
Pagellus acarne, benthopelagic, (103 g, 215 mm)	5.9	2.2	N.D.	N.D.
Uranoscopus scaber, demersal, (360 g, 273 mm)	6.2	1.4	N.D.	N.D.
Uranoscopus scaber, demersal, (184 g, 230 mm)	N.D.	1.8	N.D.	N.D.
Exocoetus volitans, pelagic-neritic, (276 g, 299 mm)	5.2	1.6	N.D.	N.D.
Scallops-Pecten Jacobaeus, benthic, 4 Kg	69.0	57.0	5.4	1.7

Table 17. Biodiversity indices of fishery tissues to be sampled in caldera [47] [48] [49].

Index	Value	Common range	Diversity/variety state
Shannon-Wiever, (<i>H'</i>)	2.874	1.50 - 3.50	Very good
Simpson's (dominance), (<i>D</i>)	0.155	0.10 - 0.25	

2.4.4. Discussion of Sea Sampling Results

The analytical reports of laboratory's physicochemical analyses of both sampling periods indicate that in sea water column samples PCBs were not detected whatsoever. PAHs & TPHs, in general, were below detectable level. The only exception appeared to be a couple of samples taken from a scuba diver, member of the scientific group, during the 2nd sampling attempt in July of 2019. In those two samples considerable quantities of TPHs and a PAH (naphthalene) was measured.

PAHs are aromatic ringed molecular structures, non-polar, derived in the coastline waters mainly from fossil marine fuels. They are hydrophobic and although generally insoluble in water, are able to be adsorbed gradually due to their affinity to organic rich sediments causing a variety of ecological negative side effects. Naphthalene detectable concentration was confirmed up to 0.601 ($\mu\text{g}\cdot\text{L}^{-1}$) (Table 15). US-EPA (1980), consolidated the toxicity of naphthalene in aquatic life [53]. Acute toxicity appears in high concentration up to 2,350 ($\mu\text{g}\cdot\text{L}^{-1}$) (LOEL)¹². Its negative effect in more sensitive species is almost certain in considerably lower concentration, though there's a lack of scientific evidence to support it [53]. Analytically the obtained results were:

C ₁₀ - C ₁₂ Fraction	35.0	$\mu\text{g}\cdot\text{L}^{-1} \pm 30.0\%$
C ₁₀ - C ₄₀ Fraction	19,300.0	$\mu\text{g}\cdot\text{L}^{-1} \pm 30.0\%$
C ₁₂ - C ₁₆ Fraction	42.1	$\mu\text{g}\cdot\text{L}^{-1} \pm 30.0\%$
C ₁₆ - C ₃₅ Fraction	10,400.0	$\mu\text{g}\cdot\text{L}^{-1} \pm 30.0\%$
C ₃₅ - C ₄₀ Fraction	8,850.0	$\mu\text{g}\cdot\text{L}^{-1} \pm 30.0\%$
Naphthalene	0.601	$\mu\text{g}\cdot\text{L}^{-1}$

PAHs are still measurable at a very close distance from the wreckage. There are certain indices/ratios (e.g. CPI¹³, n-C₁₇/n-C₃₁), which determine the n-alkane origin *i.e.* terrestrial, marine, biogenic, anthropogenic [54]. Given that PAHs were not detected in other sampling stations, a few hundred meters away at the sampling days, it is apparent that were not of local ambient biogenic origin. Consequently, the vicinity to the wreck support strongly the approach that TPHs results could be attributed to the presence of the wreckage in the area. It is accepted to the local community that sporadically the vessel "releases" marine fuel and lubricant based pollutants, prior entrapped in the vessel's interior. Underwater taken videos from the wreckage are supportive to the given interpretation. It is apparent the necessity of the continuous monitoring of the caldera marine ambient, since sporadic minor pollution events are to be expected. Nonetheless no traceable PCBs were detected whatsoever though extensive sampling took place in numerous spots in two sampling periods.

¹²Lowest Observed Effects Level.

¹³Odd to even carbon chain numbered ratio.

References in the Greek region, regarding heavy metal analyses' research in bottom sediments and pollutant indicators' estimation is considerably poor. Nonetheless, worthwhile to be mentioned, inter alia, the studies focused on mid-sized harbours' sea basins not directly comparable to our case and thus of limited value [55] [56] [57].

Regarding heavy metals concentration level in aquatic sea column, the results indicate that, apart from (Fe), only in certain locations heavy metals (Cd & Pb) were measured above the detection limit in significant concentration. (Fe) presence was by all means expected as a result of the hydrothermal sediments of the submarine volcanic activity in caldera region. Thira island is a part of the Aegean volcanic arc. Hydrothermal vents are located in-between Palea Kameni & Nea Kameni isles where (As) is measured by a factor 3 - 8 times higher than the normal seawater concentration. Additionally, located exhalation zones relatively close to the wreckage give rise to (Fe) oxides, to (Mn) (element) [58] as well as to (Fe) and (Mn) conc. in the seawater column [59].

The results derived from the two sampling periods—the 2nd sampling took place almost one month later—present a high fluctuation of heavy metals concentration in sea basin sediment and not correlated in between. Relative Percent Difference (RPD) precision assessment is adopted since duplicate sample analysis was conducted (**Table 18**). (RPD) < 20% considered to be an accepted standard rule of thumb for aqueous samples under US-EPA “Guidance on Preparing a Quality Assurance Project Plan” [60]. Relative Percent Difference (RPD) is given according to the following formula (Equation 6):

$$RPD = \frac{|\text{sample result} - \text{duplicate result}|}{(\text{sample result} + \text{duplicate result})/2} \times 100\% \quad (6)$$

Up to a certain point high fluctuation is rather explainable since the region of our interest was susceptible to side effected parameters such as the high local sea traffic (highly touristic sea channel), the environmental interaction with the relatively close distanced commercial port of “Athinio” and subsurface sea currents. Furthermore, at a close range to the wreckage area in the nearby coast, infrastructure remnants indicate the presence of an abandoned mine.

Sampling analyses in seabed sediments indicate that the Contamination Factor (CF) regarding the mid Earth (Crust), referring to (Cd) and (Pb) pollutant agents correspond to a moderate up to a very high contamination level state (CF > 6). An analogous outcome is derived by using (I_{geo}) index as regards the preindustrial period shale concentration. The modified contamination degree (mC_d) solidifies a moderate to high level contamination state. On the other hand, (PLI) indicates an overall very low contamination state.

Imbound offshore booms and in rare sampling stations (Pb) and (Ni) presence was inevitable. The only explanatory hypothesis to justify high measured values of Cd & Pb conc. in the sea column is the fate of marine oil fuel remnants which give rise to the (Ni) conc. and the ongoing physico-biochemical interaction of electrical and electronic devices of the M/S cruise with the seabed surroundings that gradually incurs degradation of the aquatic ecosystem quality.

Table 18. Relative Percent Difference criterion control over heavy metal sampling in June & July of 2019.

Sampling date	Sediment depth & location	(Cu) (mg·kg ⁻¹)	(Zn) (mg·kg ⁻¹)	(Cr) (mg·kg ⁻¹)
(5/7/2019)	(11 m)	11.3	33.3	10.1
(7/6/2019)	36°23.655N, 25°26.042E	15.5	18.3	14.3
RPD within a month		-31.3%	58.1%	-34.4%
(5/7/2019)	(100 m)	7.9	33.2	9.4
(7/6/2019)	36°23.704N, 25°25.856E	16.8	95.0	9.4
RPD within a month		-72.1%	-96.4%	0.0%
Sampling date	Sediment depth & location	(Cd) (mg·kg ⁻¹)	(Pb) (mg·kg ⁻¹)	(Ni) (mg·kg ⁻¹)
(5/7/2019)	(11 m)	2.1	49.2	15.4
(7/6/2019)	36°23.655N, 25°26.042E	N.D.	14.2	8.4
RPD within a month			110.4%	58.8%
(5/7/2019)	(100 m)	N.D.	44.8	11.6
(7/6/2019)	36°23.704N, 25°25.856E	6.4	87.2	24.1
RPD within a month			-64.2%	-70.0%
Sampling date	Sediment depth & location	(Fe) (mg·kg ⁻¹)	(Mn) (mg·kg ⁻¹)	
(5/7/2019)	(11 m)	8,450	144.0	
(7/6/2019)	36°23.655N, 25°26.042E	5,800	103.0	
RPD within a month		37.2%	33.2%	
(5/7/2019)	(100 m)	5,150	131.0	
(7/6/2019)	36°23.704N, 25°25.856E	9,150	195.0	
RPD within a month		-55.9%	-39.3%	

Steel hull plates consisting mostly of alloys Fe-Cu-Cr-Ni-Mo, according to ASTM standards, are in an advanced state to provide oxides and provoke extended ion mobilization in the seawater body. On the other hand, organotin compounds are not our case since Sea Diamond's hull was layered, already, by ecofriendly antifouling coating on an early stage. Marine HFO contains sufficient traces of V and Ni which are not measured in the seawater column.

EU Regulation No 1881/2006 sets maximum level for certain contaminants in foodstuff. When fishery products prior to consumption are the case, for the following heavy metals *i.e.* (Hg), (Cd) and (Pb) the maximum detection limits are 0.50 mg/wet kg, 0.050 mg/wet kg and 0.30 mg/wet kg respectively [61]. Fish

stock samples didn't show any seriously damaged tissues due to any kind of anthropogenic impact at close region of our interest nearby wreck. According to **Table 16**, in certain cases, (Fe), (Zn), (Mn) and (As) were resulted to be above the detected limits.

3. Hull Corrosion Evolution

Based on videos and high-quality photos taken from ROV inspection, iron plates' analysis was made along with the use of corrosion prediction computer modeling¹⁴. The scope was to be estimated the wreck condition at that time, expressed as the following introduced outcome *i.e.* as the plates' total thickness loss or the "time-to-perforation" or even the remaining thickness of the main structural plates and thereof remaining vessel's life before wiping out. "Remaining life" in our case is the time required for seawater corrosion to "consume" or corrode away the remaining thickness of the superstructure, the deck and the hull plate. In the absence of SRB¹⁵/IOB¹⁶, the remaining life is equivalent to the time-to-perforation. The time-to-perforation is the time required for localized corrosion *i.e.* pitting to perforate the remaining thickness under the worst-case scenario when SRB and/or IOB are present on the wreck.

CO₂Compass-SE (Shipwreck Edition, Version 9.18©), a commercially available computer modeling and prediction software is used to model the effects of seawater physicochemical parameters [62]. The scope of corrosion model implementation was the assessment of the structural plates situation at the inspection time given as follows:

- 1) Corrosion rate estimation of the hull plate thickness loss in (mm·y⁻¹).
- 2) Corrosion rate estimation of the superstructural thickness loss in (mm·y⁻¹).
- 3) Assessment of the effect of Zn sacrificial anode/(ICCP)¹⁷, coatings, (**Figure 12**, **Figure 13**) and the developed microorganism's film on the deterioration of the superstructure, deck and hull's plates.
- 4) Estimation of the remaining time life—in years—due to seawater corrosion phenomena, and perforation advance (consumption), to the detriment of super-structural, deck and hull's plates initial thickness.

The parameter values, assumptions and their respective values are used as inputs in CO₂Compass-SE corrosion prediction software (**Table 19**, **Table 20**). Corrosion of iron and steel in seawater is influenced by the seawater chemistry which varies with water depth [63] [64]. The shipwreck is at a water depth ranging from 86 m to 147 m, with an average depth of about 117 m. It is well established that both (DO) and temperature decrease with water depth increase in deep seas (**Figure 14**). Salinity and chlorinity are considered convertible and either parameter was required as corrosion modeling input. Hull coating is co-estimated in model prediction, since it plays a vital inhibition role to the sea

¹⁴WebCorr-Corrosion Consulting Services, Email: webcorr@corrosionclinic.com.

¹⁵Sulphate-Reducing Bacteria.

¹⁶Iron-Oxidizing Bacteria.

¹⁷Impressed Current Cathodic Protection.

corrosion advance (Figure 15 & Table 21) [65].

Results of the Corrosion Model and Discussion

The original design thickness of steel plate used for the superstructure (deck 9 and above) is 6.0 mm (Figure 15). The remaining thickness as on July the 5th (of the inspection year) was 4.86 mm. With the assumption that the seawater physicochemical parameters will not undergo significant changes in the future, the remaining superstructure (deck 9 and above) would disappear in 108 years period running from the inspection time reference and beyond. Superstructure between decks 9 to 6 (Figure 15), would disappear in 120 years and superstructure between decks 6 to 5 would disappear in 145 years.

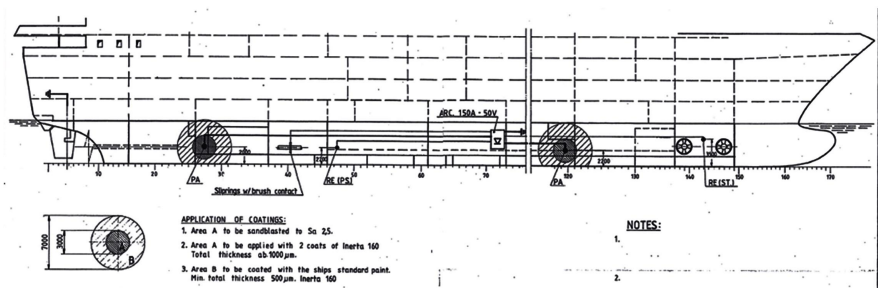


Figure 12. ICCP arrangement of Hull Plate.

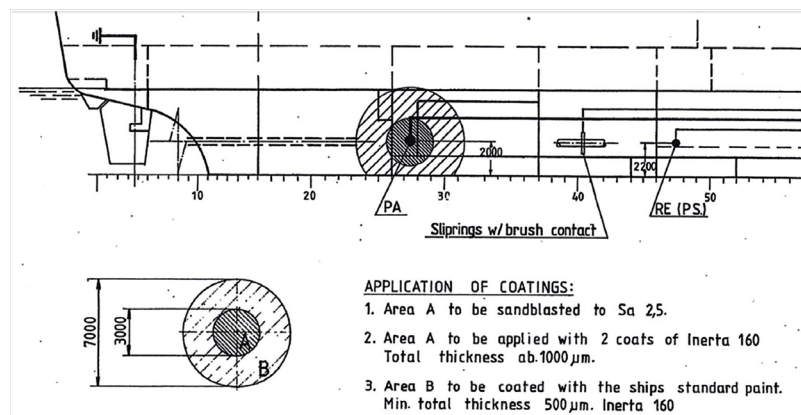


Figure 13. Coating specification for underwater hull.

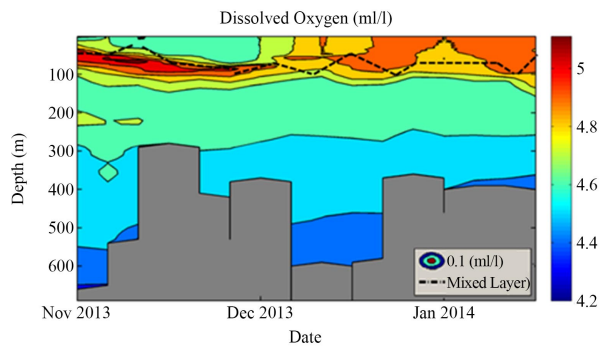


Figure 14. Dissolved oxygen decreases with water depth [66].

Table 19. List of ship's data collected and video documentation for the corrosion model (CO₂Compass-SE) implementation.**Drawings - Data - Photo Documents**

Construction Drawing, Shell (AFT)
 Construction Drawing, Shell (FORE)
 Construction Drawing, Midship Section I
 Construction Drawing, Midship Section II
 Painting Datasheet
 ICCP Drawing
 Cathodic Protection Datasheet
 Capacity Plan
 Machinery Arrangement
 Air, Overflow, and Sounding Piping Diagram
 General Plan
 Longitudinal section drawings
 Seawater physicochemical data
 ROV underwater photos and videos

Table 20. Seawater Physicochemical Parameters and assumptions at the site of Shipwreck as input data in the corrosion model.

Speed of the submarine current in the wreck area 22 to 44 (cm·sec⁻¹) (June 2019)

Surface Seawater	[pH]: 8 [Salinity]: 45.3 psu [Cl ⁻]: 25.170 mg·L ⁻¹
Seawater at depth of 103 m	[pH]: 8 [Salinity]: 44.7 psu [Cl ⁻]: 24.815 mg·L ⁻¹ [DO]: 5 - 5.5 ml·L ⁻¹ [Temperature]: 13 °C
[Age of wreck]: 12.25 years (as on 5 th of July 2019)	
[Depth]: 117 m (mean value of 86 m - 147 m)	
[DO]: 5.25 ml·L ⁻¹ (mean value of 5 - 5.5 ml·L ⁻¹)	
[Salinity]: 44.7‰	
[Current velocity]: 0.33 m·s ⁻¹ (mean value of 0.22 - 0.44 m·s ⁻¹)	
Biofilm and/or macro-fouling: present; with SRB/IOB (worst case scenario)	

Table 21. Coating systems specified for MS Sea Diamond.

Location	Type of paints	Total thickness
Weather decks	1 × 80 um Chlorinated rubber primer	240 um
	1 × 80 um Chlorinated rubber primer	
	1 × 40 um Chlorinated rubber finish	
	1 × 40 um anti slip chlorinated rubber finish	
Outside superstructure	1 × 80 um Chlorinated rubber primer	240 um
	1 × 80 um Chlorinated rubber primer	
	1 × 40 um Chlorinated rubber finish	
	1 × 40 um Chlorinated rubber finish	
Underwater hull	Ships standard paint (Inerta 160)	500 um
	Minimum total thickness 500 um	

In the presence of SRB and/or IOB microorganisms, under the worst-case scenario, localized deep pitting would have already perforated the shell plate in the superstructure from deck 9 and above. The time-to-perforation for the hull plate varies from 8 to 38 years depending on the initial design & structural thickness of the plates. There is no evidence whatsoever to indicate SRB/IOB presence on the hull at the inspection time. However, the predicted time-to-perforation under worst case scenario *i.e.* when SRB/IOB are present should be adopted when assessing the risk of the fate of toxic agents in the waterbody.

The predicted corrosion rate is estimated to be $0.07 \text{ (mm}\cdot\text{y}^{-1}\text{)}$ which implies that carbon steel structures such as hull plates, deck plates and superstructural plates have undergone 1.158 mm thickness overall loss, over the past 12.25 years due to seawater corrosion. The remaining life (from 5th of July 2019 onwards) for the 10 mm thickness plate is 208 years, meaning that the superstructure, deck and hull plates given the original design thickness of 10 mm will be consumed by seawater corrosion in 208 years (Figure 16, Figure 17). The above under the assumption of a prevailing water current velocity of $33 \text{ (cm}\cdot\text{s}^{-1}\text{)}$.

Corrosion prediction at water current velocity of $13 \text{ (cm}\cdot\text{s}^{-1}\text{)}$ in 2009 with SRB/IOB presence, indicates that the predicted remaining life of the structures due to sea corrosion is 223 year from 2009 onwards (Figure 18). Corrosion model results can be summarized below:

- Perforation of deck plates at localized spots if -and only if SRB/IOB are present (0 - 8 years)
- Perforation of superstructure at localized spots if and only if SRB/IOB are present (0 - 12 years)
- Perforation of hull plate at localized spots if and only if SRB/IOB are present (8 - 38 years)
- Collapse and disintegration of internal decks and walls (83 - 95 years)
- The loss of all structures above the hull (108 - 183 years)
- Exposure of all of heavy mechanical equipment in the bowels of the ship (e.g., boilers, turbines core parts etc.) (208 - 308 years)
- Fracturing and collapse of the hull plates (208 - 308 years)
- Exposure of the double bottom hull (295 years)
- Final extinction of the remaining resident structures (420 years and beyond)

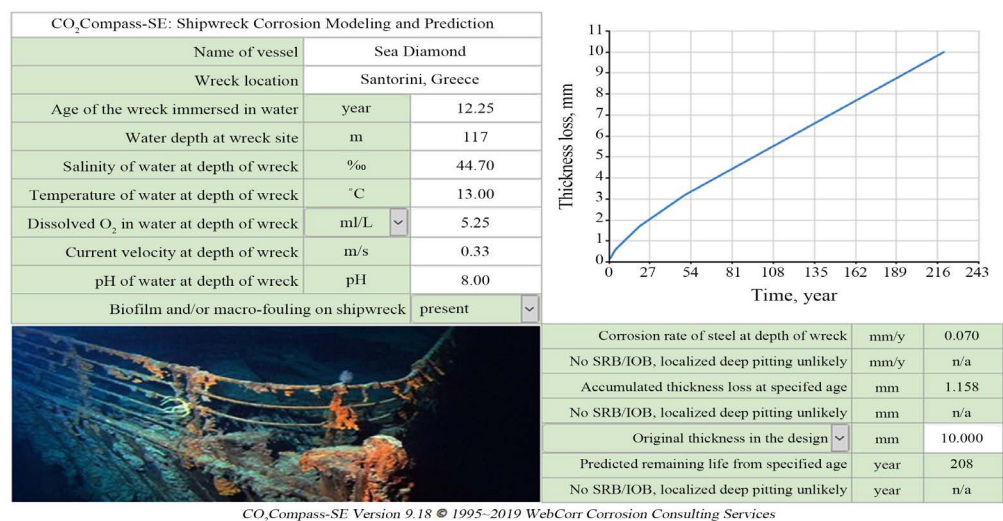


Figure 16. Prediction results when biofilm and/or macro-fouling are present but without SRB/IOB.

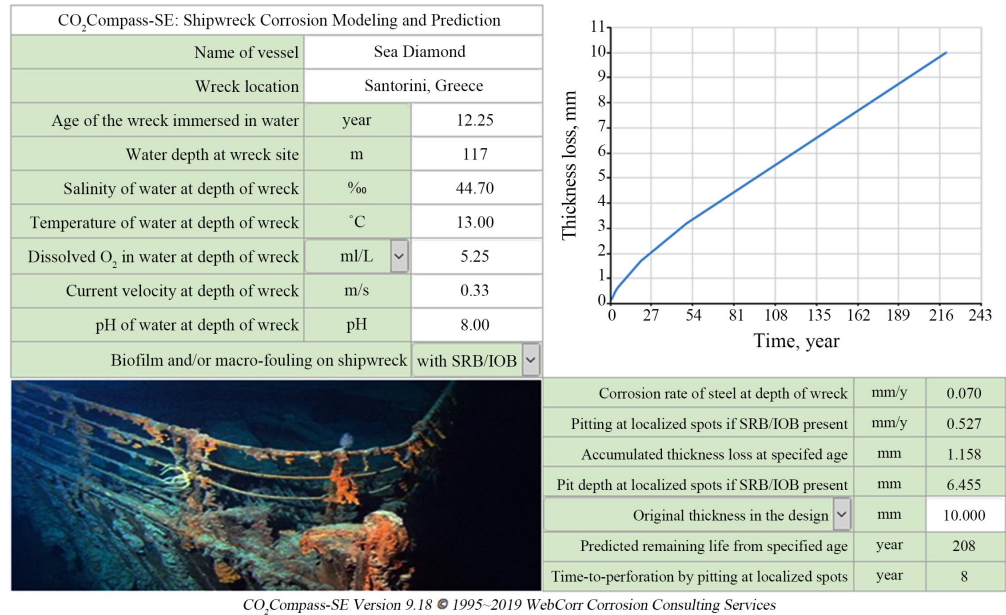


Figure 17. Prediction results when SRB/IOB are present.

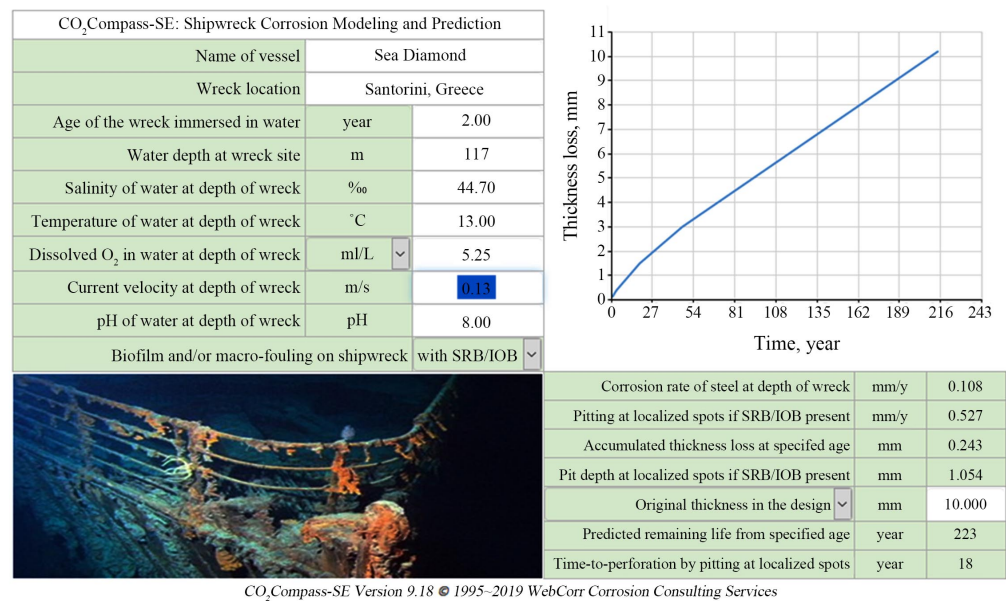


Figure 18. Corrosion prediction at water velocity of 13 (cm·s⁻¹) in 2009 with SRB/IOB presence.

4. Conclusions

According to the Appeal Court’s Decision, an environmental assessment of the water body and a judicial technical report should be conducted by a team comprised of two judicial environmentalists. They were assigned to conduct the survey, the sampling and supervise chemical analyses. Finally, they took over the obligation to compile within a time limit and file the final report.

The results of chemical analyses indicate that in a perimeter within 150 - 300 m pointing the center of an imaginary circle on the surface spot above the ves-

sel's hull stigma, heavy metals concentration detected in many predetermined sampling spots. The results were significantly higher compared to the ones of a certain sample, taken purposely from a remote spot considered it as the "reference" sample.

PAHs, TPHs are, in general, low or below detectable level in the sea column. The only exception appeared to be a couple of samples taken from a scuba diver, member of the scientific group, during the 2nd sampling attempt when considerable quantities of TPHs and a PAH (naphthalene) were measured. Given that PAHs were detected merely in one sampling station, it considered not to be of local ambient biogenic origin. The vicinity to the wreck support strongly the approach that TPHs results could be attributed to the presence of the wreckage in the area as random entrapped oil-based releases from the vessels' hull. PCBs were not detected in the sampling area.

As regards heavy metals concentration level in aquatic sea column, the results indicate that, apart from (Fe) conc. which was expected given the volcanic seabed sedimentation background, only in certain locations heavy metals *i.e.* (Pb) and (Ni) were measured above the detection limit.

Sea bed sediment sampling presents a high fluctuation of heavy metals not correlated in between which is an obstacle to draw solid conclusions. High fluctuation is rather explainable since the region of our interest was susceptible to side effected parameters such as the high local sea traffic (highly touristic sea channel), the environmental interaction with the relatively close distanced commercial port of "Athinio", subsurface sea currents and former mining activities in the near coastline.

Sampling analyses in seabed sediments indicate that the Contamination Factor (CF) regarding the mid Earth (Crust), referring to (Cd) and (Pb) pollutant agents correspond to a moderate up to a very high contamination level state ($CF > 6$) which is more or less in accordance with (I_{geo}) index as regards the preindustrial period shale concentration. The modified contamination degree (mC_d) solidifies a moderate to high level contamination state. (PLI) consolidate an overall very low contamination state.

(Pb) and (Ni) conc. were detected inbound offshore booms along with rare sampling stations. (Cd) can be justified by the dispersion and fate of marine fuel oil remnants. Steel hull plates consisting mostly of alloys Fe-Cu-Cr-Ni-Mo, according to ASTM standards, are in an advanced state to provide oxides and provoke extended ion mobilization in the seawater body. Ongoing physico-biochemical interaction of electrical and electronic devices of the M/S cruise might give rise to pollutant elements and justify considerable detected conc. Engaged heavy metal compounds, transformed into mobile complex ions incur gradually degradation of the aquatic ecosystem quality.

Organotin compounds as a part of the biocidal hull protecting layer are not our case since Sea Diamond's hull was layered, already, by ecofriendly antifouling coating on an early stage. Marine HFO contains sufficient traces of V and Ni

which are not measured in the seawater column. According to EU Regulation No 1881/2006, (Hg), (Cd) and (Pb) in fish stock samples were below the detected limits.

CO2Compass®-SE Version 9.18 software implementation for sea corrosion, predicts perforation of hull plate at localized spots providing SRB/IOB presence within (8 - 38 years) whereas the exposure of the double bottom hull is expected to occur in ~295 years period.

Acknowledgements

We gratefully thank the public local authorities of the municipality of Thira “Santorini” that supported substantially the project in accordance with the Piraeus tri-member Appeal Court board. We are also grateful to the “Topical Steering Committee for the Sea Diamond Removal” who were steadily supportive and encouraging in every way for the completion of our assignment.

Conflicts of Interest

The authors declare no conflicts of interest regarding the publication of this paper.

References

- [1] O'Brien, M. (2010) SEA DIAMOND 3 Years on... Dealing with Continual Leakage from Sunken Wrecks. *1st Adriatic Oil Spill Pollution Conference*, ITOPF, London, 14 May 2010.
<https://www.itopf.org/fileadmin/data/Documents/Papers/SeaDiamond10.pdf>
- [2] Gidarakos, E., *et al.* (2011) Reporting the Qualitative and Quantitative Characterization of Hazardous and Toxic Substances Released from the “Sea Diamond” Shipwreck-Evaluation of Current and Long-Term Impacts. Technical University of Crete, Chania.
- [3] Dimitrakakis, E., Hahladakis, J. and Gidarakos, E. (2014) The “Sea Diamond” Shipwreck: Environmental Impact Assessment in the Water Column and Sediments of the Wreck Area. *International Journal of Environmental Science and Technology*, **11**, 1421-1432. <https://doi.org/10.1007/s13762-013-0331-z>
- [4] Simbora, N., *et al.* (2008) The Impact of the Cruise Ship “Sea-Diamond” Wreckage on the Santorini Island (Aegean Sea, Eastern Mediterranean) Caldera Ecosystem. *Poster Presentation in 43rd EMBS—European Marine Biology Symposium*, University of the Azores, Ponta Delgada (Sao Miguel, Azores), Session: Marine Ecological Health Book of Abstracts, 8-12 September 2008, 120.
- [5] Simbora, N., Pancucci-Papadopoulou, M.A., Reizopoulou, S., Streftaris, N., Arvanitakis, G. and Hatzianestis, J. (2016) The Impact of the Cruise Ship “Sea-Diamond” Wreckage on the Santorini Island (Aegean Sea, Eastern Mediterranean) Caldera Benthic Ecosystem. Hellenic Centre for Marine Research.
<https://www.itopf.org/knowledge-resources/documents-guides/document/sea-diamond-3-years-on-dealing-with-continual-leakage-from-sunken-wrecks-2010/>
- [6] ISO 5667-1 (2006) Water Quality—Sampling—Part 1: Guidance on the Design of Sampling Programmes and Sampling Techniques.
- [7] ISO 5667-3 (2003) Water Quality—Sampling—Part 3: Guidance on the Preserva-

tion and Handling of Water Samples.

- [8] ISO 5667-13 (2011) Water Quality—Sampling—Part 13: Guidance on Sampling of Sludges.
- [9] ISO 5667-14 (2014) Water Quality—Sampling—Part 14: Guidance on Quality Assurance and Quality Control of Environmental Water Sampling and Handling.
- [10] ISO 5667-15 (2009) Water Quality—Sampling—Part 15: Guidance on the Preservation and Handling of Sludge and Sediment Samples.
- [11] ISO 5667-9 (1992) Water Quality—Sampling—Part 9: Guidance on Sampling from Marine Waters.
- [12] ISO 5667-12 (2017) Water Quality—Sampling—Part 12: Guidance on Sampling of Bottom Sediments from Rivers, Lakes and Estuarine Areas.
- [13] ASTM D5198-17 (2017) Standard Practice for Nitric Acid Digestion of Solid Waste.
- [14] ASTM D5358-93 (2009) Standard Practice for Sampling with a Dipper or Pond Sampler.
- [15] ASTM D5633-04 (2016) Standard Practice for Sampling with a Scoop.
- [16] ASTM D6699-16 (2016) Standard Practice for Sampling Liquids Using Bailers.
- [17] ASTM D6759-16 (2016) Standard Practice for Sampling Liquids Using Grab and Discrete Depth Samplers.
- [18] ASTM D6911-15 (2015) Standard Guide for Packaging and Shipping Environmental Samples for Laboratory Analysis.
- [19] US EPA (1996) Method 3050B: Acid Digestion of Sediments, Sludges, and Soils, Revision 2, Washington DC.
- [20] ASTM D4698-92 (2007) Standard Practice for Total Digestion of Sediment Samples for Chemical Analysis of Various Metals.
- [21] APHA 3113A, B, C. (2017) Standard Methods for the Examination of Water and Wastewater.
- [22] ISO 17852 (2006) Water Quality—Determination of Mercury—Method Using Atomic Fluorescence Spectrometry.
- [23] APHA 3111B (2005) Standard Methods for the Examination of Water and Wastewater.
- [24] ISO 11969 (1996) Water Quality—Determination of Arsenic—Atomic Absorption Spectrometric Method (Hydride Technique).
- [25] APHA 5520 B, F. (2017) Standard Methods for the Examination of Water and Wastewater, Oil & Grease.
- [26] US EPA (2010) Method 1664, n-Hexane Extractable Material (HEM; Oil and Grease) and Silica Gel Treated n-Hexane Extractable Material (SGT-HEM; Non-Polar Material) by Extraction and Gravimetry.
- [27] Czech Republic Standard, ČSN EN ISO 9377-2 (2001) Jakost vod—Stanovení uhlovodíků C10 až C40—Část 2: Metoda plynové chromatografie po extrakci rozpouštědlem.
- [28] US EPA (2003) Method 8015D (SW-846): Nonhalogenated Organics Using GC/FID, Revision 4. Washington DC.
- [29] US EPA (2000) Method 8015C (SW-846): Nonhalogenated Organics Using GC/FID, Rev. 3. Washington DC.
- [30] US EPA (1996) SW-846, Test Method 3510C: Separatory Funnel Liquid-Liquid Extraction, Part of Test Methods for Evaluating Solid Waste, Physical/Chemical Me-

- thods, Rev. 3. Washington DC.
- [31] Texas Commission on Environmental Quality (2000) TNRCC, TPH Method 1006, Characterization of NC₆ to NC₃₅ Petroleum Hydrocarbons in Environmental Samples.
- [32] Council Directive 98/83/EC (1998) The Quality of Water Intended for Human Consumption.
- [33] ISO 9377-2 (2000) Water Quality—Determination of Hydrocarbon Oil Index—Part 2: Method Using Solvent Extraction and Gas Chromatography.
- [34] ISO 6468 (1996) Water Quality—Determination of Certain Organochlorine Insecticides, Polychlorinated Biphenyls and Chlorobenzenes—Gas Chromatographic Method after Liquid-Liquid Extraction.
- [35] Din 38407-3 (1998) German standard methods for the Determination of Water, Waste Water and Sludge—Jointly Determinable Substances (Group F)—Part 3: Determination of Polychlorinated Biphenyls (F 3).
- [36] US EPA (2014) Method 8270E (SW-846): Semivolatile Organic Compounds by Gas Chromatography/Mass Spectrometry (GC-MS). Washington DC.
- [37] Czech Republic standard ČSN EN ISO 6468 (757580) (1998) Jakost Vod—Stanovení některých organochlorových insekticidů, polychlorovaných bifenyly a chlorbenzenů—Metoda plynové chromatografie po extrakci kapalina-kapalina.
- [38] US EPA (2018) SW-846 Test Method 8000D: Determinative Chromatographic Separations, Rev. 5. Washington DC.
- [39] US EPA (2007) Method 8082A: Polychlorinated Biphenyls (PCBs) by Gas Chromatography, Part of Test Methods for Evaluating Solid Waste, Physical/Chemical Methods, Rev. 1. Washington DC.
- [40] US EPA. National Recommended Water Quality Criteria—Aquatic Life, Criteria Table—Appendix A. Washington DC.
<https://www.epa.gov/wqc/national-recommended-water-quality-criteria-aquatic-life-criteria-table>
- [41] Müller, G. (1979) Schwermetalle in Sedimenten des Rheins—Veränderungen seit 1971. *Umschau*, **79**, 778-783.
- [42] Müller, G. (1981) Die Schwermetallbelastung des Neckars und seiner Nebenflüsse—Eine Bestandsaufnahme. *Chemiker Zeitung*, **105**, 157-164.
- [43] Hakanson, L. (1980) An Ecological Risk Index for Aquatic Pollution Control. A Sediment Ecological Approach. *Water Research*, **14**, 975-1001.
[https://doi.org/10.1016/0043-1354\(80\)90143-8](https://doi.org/10.1016/0043-1354(80)90143-8)
- [44] Tomlinson, D.L., Wilson, J.G., Harris, C.R. and Jeffrey, D.W. (1980) Problems in the Assessment of Heavy-Metal Levels in Estuaries and the Formation of a Pollution Index. *Helgoländer Meeresuntersuchungen*, **33**, 566-575.
<https://doi.org/10.1007/BF02414780>
- [45] Abraham, G.M.S. (2005) Holocene Sediments of Tamaki Estuary: Characterization and Impact of Recent Human Activity on an Urban Estuary in Auckland New Zealand. Ph.D. Thesis, University of Auckland, Auckland, New Zealand, 361 p.
- [46] Abraham, G.M.S. and Parker, R.J. (2008) Assessment of Heavy Metal Enrichment Factors and the Degree of Contamination in Marine Sediments from Tamaki Estuary, Auckland, New Zealand. *Environmental Monitoring and Assessment*, **136**, 227-238.
<https://doi.org/10.1007/s10661-007-9678-2>
- [47] Simpson, E.H. (1949) Measurement of Diversity. *Nature*, **163**, 688.
<https://doi.org/10.1038/163688a0>

- [48] Magurran, A.E. (2004) *Measuring Biological Diversity*. Wiley-Blackwell, Hoboken.
- [49] Shannon, C.E. and Weaver, W. (1949) The Mathematical Theory of Communication. *Science*, **185**, 27-39.
- [50] Margalef, R. (1972) Homage to Evelyn Hutchinson, or Why Is There an Upper Limit to Diversity. *Transactions of the Connecticut Academy of Arts and Sciences*, **44**, 211-235.
- [51] Krebs, C.J. (1999) *Ecological Methodology*. 2nd Edition, Benjamin Cummings, Menlo Park, CA.
- [52] Washington, H.G. (1984) Diversity, Biotic and Similarity Indices: A Review with Special Relevance to Aquatic Ecosystems. *Water Research*, **18**, 653-694.
[https://doi.org/10.1016/0043-1354\(84\)90164-7](https://doi.org/10.1016/0043-1354(84)90164-7)
- [53] US EPA (1980) *Ambient Water Quality Criteria for Naphthalene*. Washington DC.
<https://www.epa.gov/sites/production/files/2019-03/documents/ambient-wqc-naphthalene-1980.pdf>
- [54] Fingas, M. (2015) *Handbook of Oil Spill Science and Technology*. 2nd Edition, John Wiley & Sons, Hoboken. <https://doi.org/10.1002/9781118989982>
- [55] Papaefthymiou, H., Papatheodorou, G., Geraga, M., Moustakli, A. and Kapos, J. (2010) Elemental Concentrations in Sediments of the Patras Harbour, Greece, Using inAA, ICP-MS and AAS. *Microchemical Journal*, **96**, 269-276.
<https://doi.org/10.1016/j.microc.2010.04.001>
- [56] Poulos, S., Alexandrakis, G., Karditsa, A. and Drakopoulos, G.P. (2007) Heavy Metal Investigation as Pollutant Indicators in Bottom Sediments in the Harbours Heraklion and Alexandroupolis (Aegean Sea, Greece). *Proceedings of the 10th International Conference on Environmental Science and Technology*, Kos Island, Greece, 5-7 September 2007, B634-B641.
- [57] Violintzis, C., Arditoglou, A. and Voutsas, D. (2009) Elemental Composition of Suspended Particulate Matter and Sediments in the Coastal Environment of Thermaikos Bay, Greece: Delineating the Impact of Inland Waters and Wastewaters. *Journal of Hazardous Materials*, **166**, 1250-1260.
<https://doi.org/10.1016/j.jhazmat.2008.12.046>
- [58] Boström, K. and Widenfalk, L. (1984) The Origin of Iron-Rich Muds at the Kameni Islands, Santorini, Greece. *Chemical Geology*, **42**, 203-218.
[https://doi.org/10.1016/0009-2541\(84\)90015-9](https://doi.org/10.1016/0009-2541(84)90015-9)
- [59] Varnavas, S.P. and Cronan, D.S. (2005) Submarine Hydrothermal Activity off Santorini and Milos in the Central Hellenic Volcanic Arc: A Synthesis. *Chemical Geology*, **224**, 40-54. <https://doi.org/10.1016/j.chemgeo.2005.07.013>
- [60] US EPA. Project Plan Development Tool: Module 1: Guidance on Preparing a Quality Assurance Project Plan.
<https://www.epa.gov/sites/production/files/2015-06/documents/module1.pdf>
- [61] Commission Regulation (EC) No. 1881/2006 Setting Maximum Levels for Certain Contaminants in Foodstuffs.
- [62] CO2Compass-SE (2018) (Version 9.18), User's Manual.
- [63] Schumacher, M.M. (1979) *Seawater Corrosion Handbook*. Noyes Data Corporation, Park Ridge, NJ, 150.
- [64] Winston Revie, R. (2011) *Uhlig's Corrosion Handbook*. 3rd Edition, John Wiley & Sons, Hoboken.
- [65] Cramer, S.D. and Covino Jr., B.S. (2006) *ASM Handbook Vol.13C Corrosion: En-*

vironments and Industries. ASM International, Ohio.

<https://doi.org/10.31399/asm.hb.v13c.9781627081849>

- [66] Kassis, D., Krasakopoulou, E., Korres, G., Petihakis, G. and Triantafyllou, G.S. (2016) Hydrodynamic Features of the South Aegean Sea as Derived from Argo T/S and Dissolved Oxygen Profiles in the Area. *Ocean Dynamics*, **66**, 1449-1466. <https://doi.org/10.1007/s10236-016-0987-2>